



Code–code comparisons of DIVIMP's 'onion-skin model' and the EDGE2D fluid code

P.C. Stangeby^{a,b,*}, J.D. Elder^a, W. Fundamenski^a, A. Loarte^{a,b}, L.D. Horton^{a,b},
R. Simonini^{a,b}, A. Taroni^{a,b}, O.F. Matthews^{a,b}, R.D. Monk^{a,b}

^a Institute for Aerospace Studies, University of Toronto, 4925 Dufferin Street, North York, Ont., Canada, M3H 5T6

^b JET Joint Undertaking, Abingdon, Oxon, UK

Abstract

In onion-skin modelling, O-SM, of the edge plasma, the cross-field power and particle flows are treated very simply e.g. as spatially uniform. The validity of O-S modelling requires demonstration that such approximations can still result in reasonable solutions for the edge plasma. This is demonstrated here by comparison of O-SM with full 2D fluid edge solutions generated by the EDGE2D code. The target boundary conditions for the O-SM are taken from the EDGE2D output and the complete O-SM solutions are then compared with the EDGE2D ones. Agreement is generally within 20% for n_e , T_e , T_i and parallel particle flux density Γ for the medium and high recycling JET cases examined and somewhat less good for a strongly detached CMOD example.

Keywords: SOL plasma; Divertor plasma; 1D model; 2D model; Fluid simulation

1. Introduction

There are two different approaches employed to model the edge plasma. The first is the 2D fluid codes, such as EDGE2D [1], where the boundary conditions are specified at the upstream end of the SOL. Typically, the electron density on the separatrix at the outside mid-plane and the power inflow are specified. The cross-field transport coefficients D_{\perp} , χ_{\perp}^e , χ_{\perp}^i and v_{pinch} must also be specified. The second approach is the 'onion-skin models', O-SM [2–6], where boundary conditions n_e , T_e , T_i are specified across the divertor targets, ideally from experiment. One then employs *one-dimensional* models, based usually on the three conservation equations, to construct *two-dimensional* solutions giving n_e , T_e , T_i plasma flow velocity and parallel electric field, everywhere throughout the edge. The cross-field transport coefficients are not needed in this approach; however, they are *implicit* in the boundary conditions specified across the targets and so can, in principle, be *extracted* from O-SM analysis. The O-SM

approach is attractive for interpretive modelling of edge experimental data and O-S Models have generally been the basis for work with the LIM [2] and DIVIMP [6] interpretive impurity codes.

2. Can the crude assumptions about cross-field flows in O-S modelling be justified?

O-S modelling cannot avoid making assumptions about cross-field flows. For each particular SOL flux tube, the power flow to the target and the power to supply any volume sinks in that tube must have entered that flux tube at some point. Where did the input power P_{in} enter that flux tube? In reality, the cross-field heat source is distributed spatially in a rather complex way, dependent on the local cross-field second derivatives of temperature and density and the (possibly locally varying) values of D_{\perp} , $\chi_{\perp}^{e,i}$. In 2D fluid modelling usually D_{\perp} , $\chi_{\perp}^{e,i}$ are assumed to be spatially constant, but since the cross-field flows are solved for in a self-consistent way, that still results in spatially complicated flow patterns.

In O-S modelling, at least in basic form, all of this complexity is replaced by simple assumptions e.g. that the

* Corresponding author.

heat inflow P_{in} is assumed to enter at the upstream end, or uniformly along the tube etc. These assumptions are so simple that it raises a fundamental question about the validity of the O-SM approach: *can a reasonable edge plasma solution still be expected when cross-field transport is treated so simply?* The present paper addresses this specific question about O-S modelling by taking target conditions calculated by the EDGE2D fluid code, together with the usual crude O-SM assumptions about cross-field flows and comparing the resulting 2D O-SM solutions with the EDGE2D ones. The parallel physics is kept essentially the same in the O-SM as used in EDGE2D and so one is able to examine directly the consequences of treating the cross-field flows so differently.

3. Including neutral hydrogen modelling in O-S modelling

In the simplest O-S models the spatial distribution of the hydrogenic ionization is treated simply. The total ionization in each flux tube is taken to be equal to the ionic outflow to the target (which is known from the boundary conditions). The spatial distribution of ionization is imposed in some approximate way i.e. by specifying the characteristic ionization length along the tube. In such cases no assumption is required about the spatial distribution of crossfield particle flows.

In more sophisticated O-S models, iteration is used, coupling the plasma solver with a neutral code such as NIMBUS [7], etc. On the first pass, a ‘starter plasma’ is generated using the O-SM plasma solver and some ad hoc ionization source, or perhaps a ‘seed plasma’ is used, e.g. from an EDGE2D output. Once a full 2D plasma background has been generated (or imported) NIMBUS is called and the spatial distribution of ionization is then available for the next pass with the O-SM plasma solver. Iteration between NIMBUS and the plasma solver continues until the solution stops evolving, which usually occurs in a few passes. The benefits to this approach are:

(a) The ad hoc assumption about ionization distribution is replaced by a more self-consistent one. The ionization distribution largely controls the plasma flow velocity, parallel convection and the friction force on impurities.

(b) Flow reversal is naturally included. Ionization on a flux tube in excess of the ionic target flow implies flow reversal away from the target, starting at a point, typically slightly upstream of the target [8], with this excess of particles being ‘drained off’ by cross-field transport. Other flux tubes, experiencing an ionization deficit, are fed particles by these cross-field flows and can have high flow velocities toward the target over great lengths.

(c) Volume energy sources/sinks for electrons and ions associated with neutrals can be included (through iteration). These include the energy loss by electrons due to excitation, dissociation and ionization; energy gain/loss for ions due to charge exchange, ionization etc.

Regardless of how the ionization is modelled, the issue remains: how crude can one afford to be in the O-SM assumptions about the cross-field particle flows? Two assumptions have been used here to distribute the excess particles for the flow-reversed tubes: (a) a spatially-constant cross-field sink of just enough strength to ‘drain off’ all the excess particles and (b) the same, but sink proportional to local n_e , presumably more realistic. Either method is implemented as part of the iteration process. The cross-field source for tubes ‘in deficit’ is taken here to be spatially uniform.

4. Onion-skin model assumptions used

NIMBUS was used to provide 2D hydrogenic ionization and electron and ion volume power terms associated with neutrals. The three conservation equations were used. Particle balance included recombination (only 2-body here, as that was the assumption in these EDGE2D runs). As in the EDGE2D runs, a fraction of the target ionic flow could be removed (pumped) and replaced (in EDGE2D) by ionic inflow from the core into the SOL (for the O-SM these removed particles were automatically replaced by the cross-field source/sink mechanism described earlier which insured particle balance for each tube). Momentum balance included i–n friction calculated (as in EDGE2D) using the NIMBUS-values for the local neutral density and neglecting neutral drift velocity. No impurity radiation, as in these EDGE2D cases. Sonic target flow was assumed, as in EDGE2D. Each half-tube (from target to midway along the SOL to next target) was treated separately, thus at the mid-point discontinuities in n , T_e , T_i result; flow velocity zero at mid-point.

5. A ‘moderate’ recycling JET case

For truly low recycling (‘sheath limited’) conditions, since there are no temperature variations along the SOL, the O-SM approach works, trivially. The first case considered here is therefore one of ‘moderate’ recycling i.e. with T -variations along the SOL of a factor 3 or so. This JET case is a rather ‘ordinary’ plasma: target T about 30 eV at the separatrix; maximum target n about 10^{19} m^{-3} . The EDGE2D input assumptions: input power of 0.5 MW to e and i channels; $\chi_{\perp}^e = \chi_{\perp}^i = 1 \text{ m}^2/\text{s}$ and $D_{\perp} = 0.1 \text{ m}^2/\text{s}$. Outside midplane on separatrix: $T_e \approx 50 \text{ eV}$, $T_i \approx 90 \text{ eV}$ and $n_e \approx 7 \times 10^{18} \text{ m}^{-3}$. The O-SM followed T_e and T_i separately, neglecting equipartition, otherwise as described earlier. The O-SM ‘starter plasma’ assumed an arbitrary analytic ionization distribution, but the solution quickly iterated to an unvarying solution; 4 iterations were used, but the solution ‘settled down’ almost immediately. P_{in} distributed uniformly.

Sample results are shown in Figs. 1 and 2. There were

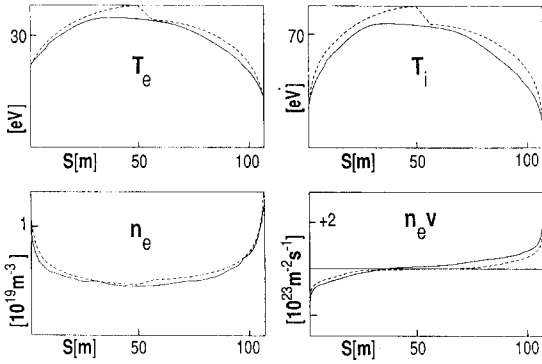


Fig. 1. ‘Moderate recycling’ JET case. 4th SOL grid ring from separatrix (2 cm from separatrix, on target). n_e , T_e , T_i , $\Gamma (=nv)$ as functions of s , measured along \vec{B} from outer target (left end) to inner target (right). Solid line: EDGE2D. Dashed line: onion-skin model. P_{in} uniform.

14 SOL grid rings for this particular mesh. Fig. 1 shows $n_e(s)$, $T_e(s)$, $T_i(s)$, $\Gamma(s)$ ($\Gamma \equiv nv$) for the 4th SOL ring from the separatrix, Fig. 2 for the 8th SOL ring, where s is measured along \vec{B} , target-to-target. In all such plots shown here, the outer target is at the left side and the inner at the right side. Agreement between the O-SM and EDGE2D solutions was generally to within $\leq 20\%$ for the 4 quantities on all SOL rings. The largest T_e variation along any ring was $\sim 3 \times$; $T_i \sim 5 \times$.

6. Extracting D_{\perp}^{SOL} , $\chi_{\perp}^{\text{SOL}}$ from the profiles

One application of O-S modelling is the extraction of D_{\perp}^{SOL} and $\chi_{\perp}^{\text{SOL}}$ from the calculated 2D n and T profiles [3–5]: one has all the volume and target power and particle fluxes, also all the cross-field n and T gradients, therefore straightforward balance calculations can extract D_{\perp}^{SOL} and $\chi_{\perp}^{\text{SOL}}$. By carrying out the balance-calculations for different portions of the SOL one can extract D_{\perp}^{SOL} and $\chi_{\perp}^{\text{SOL}}$ as a function of r . One can therefore extract D_{\perp}^{SOL} and

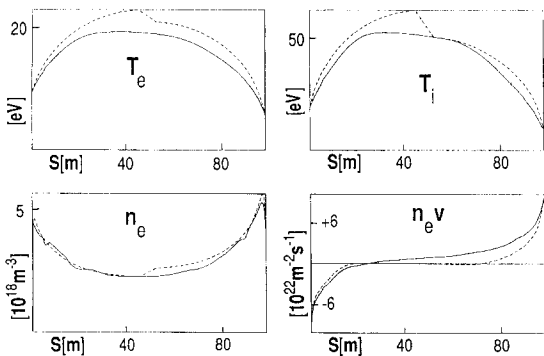


Fig. 2. As for Fig. 1 but 8th SOL grid ring (4 cm from separatrix, on target).

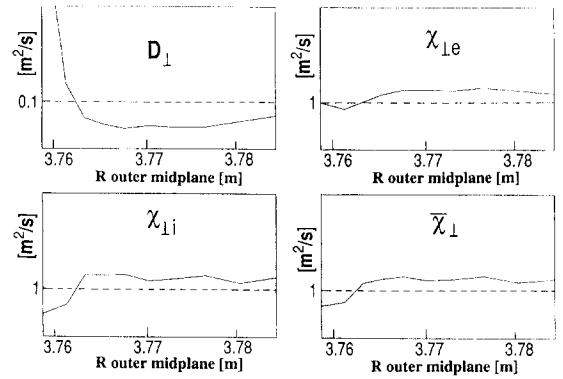


Fig. 3. Extracted D_{\perp} , χ_{\perp} for ‘moderate recycling’ JET case. Transport coefficients from the 2D onion-skin model solutions (e.g. Figs. 1 and 2), (solid lines) as a function of ring location at the outside midplane. EDGE2D input values, dashed.

$\chi_{\perp}^{\text{SOL}}$ essentially from experimental data, when the O-SM boundary conditions are taken from experiment. Here we wish to use the extraction procedure as a further test of the quality of matching of the O-SM solution to the EDGE2D one. This is a more demanding test since it is based, in part, on matching radial gradients of n and T . It is also not always possible to extract D_{\perp}^{SOL} : under some circumstances each flux tube is largely supplied by local ionization and cross-field particle flows can be too small to allow reliable extraction of D_{\perp}^{SOL} . A similar problem does not arise for $\chi_{\perp}^{\text{SOL}}$ since the power source for the SOL is always the core.

Fig. 3 shows the values of D_{\perp}^{SOL} , $\chi_{\perp e}^{\text{SOL}}$, $\chi_{\perp i}^{\text{SOL}}$, $\bar{\chi}_{\perp}^{\text{SOL}}$ as a function of r (measured at the outer midplane) extracted from the O-SM 2D solutions and compared with the EDGE2D input assumptions. Agreement is to within a factor of 2 or better. $\bar{\chi}_{\perp}^{\text{SOL}}$ used combined i and e power balances. The volume power terms were used in the extraction. By extracting D_{\perp}^{SOL} first, cross-field convection could be included in the power balance to extract $\chi_{\perp}^{\text{SOL}}$; the D_{\perp}^{SOL} value extracted in this case was expected to be reasonably reliable (NIMBUS calculations showed that about 10% of the neutrals were ionized inside the separatrix, which provides a reasonably strong cross-field particle flow).

7. A ‘high recycling’ JET case

A second JET case involved low/moderate recycling near the separatrix, where target $T \sim 50$ eV, $n \sim 2 \times 10^{19} \text{ m}^{-3}$, but by the 8th ring out, on the inside, the target T_c had dropped to 2.6 eV, T_i to 4.1 eV and $n = 2 \times 10^{19} \text{ m}^{-3}$, giving ‘high recycling’ conditions there, or more correctly, large parallel T -gradients. The EDGE2D input assumptions were as before, but now with 2 MW input to e and i power channels, 5% target ion pumping. Upstream

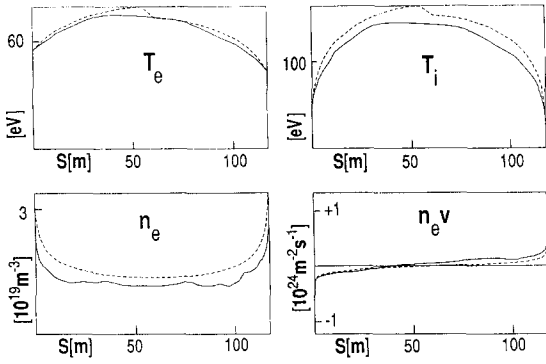


Fig. 4. ‘High recycling’ JET case. As for Fig. 1 but for 2nd SOL grid ring (6 mm from separatrix, on target). A ring with small parallel temperature gradient. P_{in} uniform.

separatrix: $n_e = 1.4 \times 10^{19} \text{ m}^{-3}$, $T_i = 144 \text{ eV}$, $T_e = 86 \text{ eV}$. The O-SM was iterated five times. P_{in} was uniform. Figs. 4 and 5 show results for the 2nd ring (moderate T -rise) and for the 8th ring (large T -rise). For the latter ring, on the inside, the T_e -rise is by $9.2 \times$ for EDGE2D and $10.6 \times$ for O-SM; T_i -rise is by $15.9 \times$ for EDGE2D and $12.2 \times$ for O-SM. Match between the O-SM and EDGE2D solutions was overall slightly less than for the first case, but was still generally $\leq 20\%$. The extracted value $\bar{\chi}^{SOL}$ was close to the EDGE2D input value, but D_{\perp}^{SOL} could not be extracted for this high recycling case.

8. A detached CMOD case

Detached divertor cases are the most challenging ones encountered to date. Indeed it is not evident that the O-SM approach can work for detachment, at least when the boundary conditions are at the target and the O-SM calculation proceeds upstream: if the plasma completely detaches so that all plasma contact at the target ceases, it would be impossible to use the basic O-SM approach

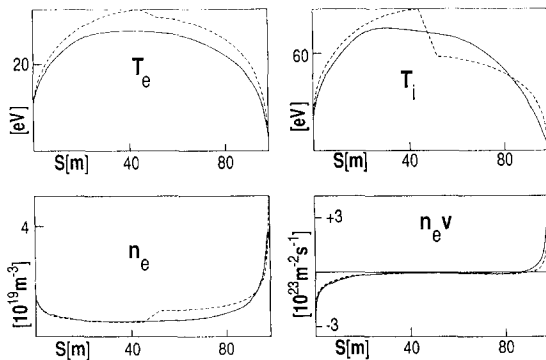


Fig. 5. As for Fig. 4 but for 8th SOL grid ring. A ring with large parallel temperature gradients.

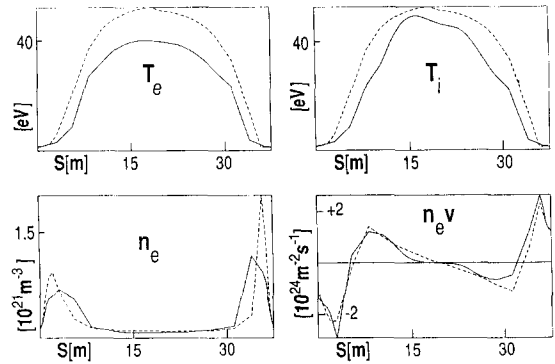


Fig. 6. Detached CMOD case. As for Fig. 1 but for 1st SOL grid ring. P_{in} uniform above X-point.

discussed here. For purposes of the present study, however, we focus on the specific question of whether the crude treatment of cross-field flows used in O-S modelling is acceptable and we address that question now in the context of detachment, also for a case where not all plasma contact with the target is lost.

Detachment was simulated in CMOD using ‘power starvation’ in an EDGE2D run: only 0.1 MW (each) was input to the e and i channels; 5% ion target pumping; $\chi_{\perp e}^{SOL} = \chi_{\perp i}^{SOL} = 0.3 \text{ m}^2/\text{s}$ and $D_{\perp}^{SOL} = 0.07 \text{ m}^2/\text{s}$. Upstream separatrix: $n_e = 7 \times 10^{19} \text{ m}^{-3}$, $T_e = 37 \text{ eV}$ and $T_i = 45 \text{ eV}$. At the separatrix strong detachment resulted at both targets: $T_e = 0.7 \text{ eV}$, $T_i \sim 1 \text{ eV}$ and $n_e \sim 1.4 \times 10^{20} \text{ m}^{-3}$, i.e. a pressure-drop along the SOL of $\approx 12 \times$, Fig. 6. By the 6th ring out, the pressure drop was only $3.6 \times$, although target temperatures were still $\sim 1 \text{ eV}$, Fig. 7.

In attempting to match this EDGE2D solution, it became clear that unless the parallel physics in the O-SM was very close to that in EDGE2D, including all the volume sinks/sources, then quite different O-SM and EDGE2D solutions could result. O-SM atomic physics options were developed to match as closely as possible those which had been used in the EDGE2D run which

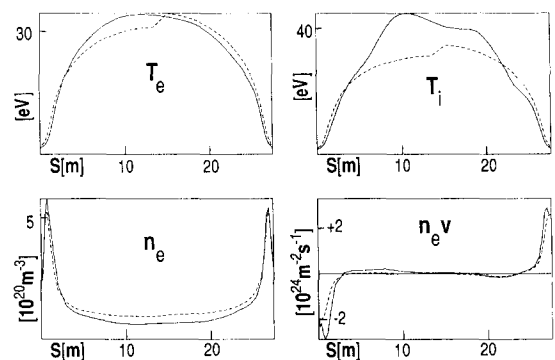


Fig. 7. As for Fig. 6 but for 6th SOL grid ring (15 mm from separatrix, on target).

involved significant assumptions and approximations. In order to ensure that the volume sources/sinks associated with hydrogenic recycle were identical in the O-SM, as the EDGE2D run, they were calculated by applying NIMBUS to the EDGE2D 2D plasma. P_{in} was uniform above the X-point (for P_{in} at mid-point, the maximum T_e was $\sim 10\%$ higher). The O-S model used a combined ion and electron power equation (single T) and for the results shown, assumed that excess ionization occurring on any flux tube was ‘drained off’ at a rate proportional to local n_e (a uniform sink gave modest differences on some rings). One may note the characteristic features of strong detachment: a density spike standing away from the target with T rather low and constant there. Near the separatrix, flow reversal is strong, see $\Gamma(s)$ plots, Fig. 6.

The match between O-SM and EDGE2D is less good than before but was better than a few 10% for most quantities on most rings. It was found that if the O-SM solution was allowed to evolve through iteration, then it diverged significantly from the EDGE2D solution. The O-SM did not precisely mimic the parallel and atomic physics used in EDGE2D, for example, ion loss to walls, with associated recycle, was included in EDGE2D but not the O-SM and such differences may be the cause of the divergence of iterated solutions. While the detached solutions obtained, non-iterated or iterated, were quite sensitive to precisely what *parallel* (including atomic) physics assumptions were made, the sensitivity to how *cross-field* flows were distributed was not great. Therefore, regarding the objective of the present study, it was concluded that detached plasmas appear to be similar to attached ones in this insensitivity.

9. Conclusions

For the ‘medium/high’ recycling and detached examples considered, the O-SM solutions match the EDGE2D ones throughout the SOL to levels $\leq 20\%$ for the most part and therefore to better than what can be experimentally resolved. It appears, therefore, that edge solutions may not be significantly sensitive to the details of how cross-field flows of power and particles are distributed along the SOL and that the simple way that onion-skin modelling handles such flows can be acceptable. Future studies will focus on identifying more precisely the plasma regimes for which fully-iterated O-SM solutions can be obtained, also the regimes for which D_{\perp} can be reliably extracted from an O-SM.

References

- [1] R. Simonini, G. Corrigan, G. Radford, J. Spence and A. Taroni, *Contrib. Plasma Phys.* 34 (1994) 368.
- [2] P.C. Stangeby, C. Farrell, S. Hoskins and L. Wood, *Nucl. Fusion* 28 (1988) 1945.
- [3] K. Shimizu, K. Itami, H. Kubo et al., *J. Nucl. Mater.* 196–198 (1992) 476.
- [4] R.D. Monk, L.D. Horton, A. Loarte et al., *J. Nucl. Mater.* 220 (1995) 612.
- [5] B. LaBombard, *Phys. Plasmas* 2 (1995) 2242.
- [6] P.C. Stangeby and J.D. Elder, *J. Nucl. Mater.* 196–198 (1992) 258.
- [7] E. Cupini, A. De Matteis and R. Simonini, *NET Rept. EUR XII* (1984) 324/9.
- [8] G.P. Maddison, D. Reiter, P.C. Stangeby and A.K. Prinja, in *Proc. 20th EPS Conf on Controlled Fusion and Plasma Phys.*, Lisboa, July 26–30, 1993, II-779 and references therein.